

PALAIOS, 2021, v. 36, 216–224 Research Article DOI: http://dx.doi.org/10.2110/palo.2021.004



X-RAY TOMOGRAPHIC MICROSCOPY AS A MEANS TO SYSTEMATICALLY TRACK EXPERIMENTAL DECAY AND FOSSILIZATION

TARA SELLY^{1,2} AND JAMES D. SCHIFFBAUER^{2,1}

¹X-ray Microanalysis Core Facility, University of Missouri, 101 Geological Sciences Building, Columbia, Missouri 65211, USA
²Department of Geological Sciences, University of Missouri, 101 Geological Sciences Building, Columbia, Missouri 65211, USA email: sellyt@missouri.edu

ABSTRACT: Laboratory-based decay experiments have become commonly used to supplement our understanding of how organisms enter the fossil record. Differences in how these experiments are designed and evaluated, however, including dissimilarities in qualitative decay-scoring indices superimposed on variability in model organisms, renders any semblance of comparison between studies unreliable. Here, we introduce the utility of X-ray tomographic microscopy (µCT) as a means for reliable and repeatable analysis of soft-tissue decay experiment products. As proofof-concept, we used a relatively simple experimental design with classic studies as comparators, and present our analytical protocol using µCT for capturing the entire volume of the decay subject. Segmentation software then allows for 3D volume analysis and high-resolution internal and external character identification. We describe the workflow from sample preparation, contrast-staining, and data collection to processing and analysis of the resulting data, using peppermint shrimp (Lysmata wurdemanni) as model organisms, and compare our results to previous taphonomic studies. These methods allow for improved visualization and quantification of decay and internal volume analysis with minimal handling as compared to traditional qualitative scoring methods. Using the same scoring criteria as previous studies, this study revealed similar decay results for certain features, while we were additionally able to detect other feature loss or alteration earlier—importantly without need for potentially distortive sample handling. We conclude that μ CT is a more effective, straightforward, and exact means for extracting quantitative data on the progression of decay and should be adopted in future studies, where available, to streamline and standardize comparisons.

INTRODUCTION

While the vast majority of the fossil record is represented by bones, teeth, shells, and other hard or skeletal materials, fossils of soft tissues do occur, but typically require a specific suite of conditions—for instance including anoxia, minimal disturbance, delayed degradation, and either permineralization or replacive authigenic mineralization (e.g., Briggs 2003). These rare cases of soft-tissue preservation can be thought of as a balancing act between organismal decay and mineralization—processes that can often be better appreciated by observing decay of modern analogues. For this reason, decay experimentation has become a common proxy for understanding how ancient life may have entered the fossil record. Indeed, experiments that track organismal decay have provided crucial information towards identifying mechanisms that facilitate fossil preservation as well as biases that are inherent in the interpretation of fossils (Behrensmeyer and Kidwell 1985; Briggs 1995; Sansom et al. 2010)

Generally, factors that contribute to the preservation of soft tissues can be divided into two categories: (1) those that facilitate preservation by delaying or deterring tissue decay, and (2) those that promote mineralization, although commonly at the expense of the tissues being preserved (Cai et al. 2012; Schiffbauer et al. 2014; Purnell et al. 2018). Numerous previous studies have employed taphonomic experiments to help parse the relative importance of such factors that improve the likelihood of preservation, for instance including microbial activity, sediment chemistry, and redox conditions (e.g., Briggs and Kear 1994; Darroch et al. 2012; Wilson and Butterfield 2014; Gibson et al. 2018; see also review by Sansom 2014). Regardless of the experimental protocol and

the conditions being evaluated, data collection and subsequent analyses in many of these studies have relied upon somewhat subjective evaluations, such as visual appraisals and qualitative decay indices, although statistical approaches to data assessment and/or chemical analyses are not uncommon. With regard to qualitative decay indices, these methods often record either presence/absence data or the assignment of arbitrary values, and thus their applicability for comparison across different studies is limited. Further, sometimes simple visual assessment can be challenging. For example, substrate composition and permeability are commonly important factors in these experiments (Wilson and Butterfield 2014), but removing the organism from its sediment matrix for evaluation can be difficult, damaging, and potentially alter results and interpretations. For decay experimentation to ultimately become more valuable to taphonomists, we must be able to examine a wide range of fossilization factors and model organisms but also limit the variability in product analysis that makes between-study comparisons incompatible and unreliable.

Undeniably, as decay experiments have grown in popularity, finding a means to systematize data collection and analysis has become a vital step towards improving their applicability. To this end, establishment of standardized protocols should focus on providing repeatability and a common, but improved, mode of comprehensive visualization of decay products, which will result in more directly comparable datasets. With increasing availability of X-ray tomographic microscopy (μ CT), and its emergent use in paleobiological studies, it is perhaps surprising that very few experimental decay studies have taken advantage of this technology (or similar volume imaging techniques) for observing the sequence of decay

Published Online: June 2021

Copyright © 2021, SEPM (Society for Sedimentary Geology) 0883-1351/21/036-216

(e.g., Iniesto et al. 2015; McCoy et al. 2015; Fordyce et al. 2020; Mähler et al. 2020)

Herein, as a proof-of-concept approach, we seek to establish a novel protocol using µCT and three-dimensional (3D) visualization methods to more systematically track decomposition as compared to past-used methods. Among other benefits, this method allows for quantification of volumetric changes that could be coupled with changes in replicate weight during the course of the experiment, for example, and thus lowers our reliance on subjective indices. With appropriate sample preparation, which is reasonably minimal, µCT provides a nondisruptive view of both external and internal anatomical features. Specific features or anatomical structures of interest can be isolated and analyzed via the application of 3D visualization software. In experiments promoting induced mineralization, these techniques can also provide in situ observation of mineral nucleation and growth (McCov et al. 2015; Mähler et al. 2020), whereas taphonomic mineralization in most other previous studies has been inferred after cessation of the experiment, via chemical analysis of encasing sediments (e.g., Darroch et al. 2012; Gibson et al. 2018) or by destruction of the decay subject (Briggs and Kear 1993). Thus, perhaps a broader advantage is that full-volume 3D datasets can be shared between researchers interested in comparing results or focusing on different aspects of anatomical decay or mineralization. With selected time slices important to the design of the study, a time-series of the progression of decay (in our case using different replicates) can be captured over the duration of the experiment. By permitting direct visualization of such features as mineral replication, quantitative assessments of volume retention and loss, and nondestructive views onto the presence or absence of otherwise obscured internal anatomical structures, our approach holds vast potential to improve the appraisal of decay and provides an integral step towards comparability between studies with analogous decay subjects.

PREVIOUS APPROACHES

To better ground-truth our observations with previous decay-experiment approaches, the resulting data from this study were compared to reports from two previously published and comparable studies: (1) Briggs and Kear (1994) was chosen as a classic example of experimental taphonomy in the literature, using caridean shrimp as decay subjects; and (2) Klompmaker et al. (2017) was chosen as a more recent examination of crustacean decay. The fundamental difference between these studies is that Briggs and Kear (1994) used isolated decay vessels where atmospheric composition and diffusion rates were of primary importance, whereas Klompmaker et al. (2017) used flow-through tank settings with minimal-to-no sample handling or artificial disturbance in an effort to observe preservation potential of varying crustaceans in unmanipulated environments. Other protocol details of these two studies are provided below.

Briggs and Kear 1994

In the Briggs and Kear (1994) decay study, two caridean shrimp taxa, *Crangon crangon* and *Palaemon* sp., were used to assess morphological changes of organic structural tissues (carapace) at varying oxygenic conditions at the onset of the experiment in both open and closed systems. The amount of oxygen in the artificial seawater was varied in six ways (see their figure 2): (la) starting oxygen 50% saturation, re-oxygenation by rapid diffusion; (lb) starting oxygen 50% saturation, re-oxygenation by slow diffusion; (1c) starting oxygen 50% saturation, no diffusion; (1d) completely anoxic; (le) starting oxygen 50% saturation, diffusion from partially oxygenated air space; (1f) no oxygen, diffusion from partially oxygenated air space. Other variables were also assessed, including some buried replicates and variation of phosphate and bicarbonate concentrations in the artificial seawater. To assess decay, a qualitative decomposition

sequence, enumerated from 0 to 5, was ascribed by changes in morphology as follows: (0) freshly killed; (1) swollen; (2) ruptured; (3) hollow; (4) disarticulated; and (5) fragmented. All organisms were euthanized by anoxia and a wet weight was measured. Specimens were placed on the bottom of a glass container with artificial seawater. Specimens were observed approximately weekly for up to 75 weeks, though most data visualization included in this publication views only up to week 8 of the experimentation. At each observation interval, the specimen was viewed and photographed within the decay container. If a bacterial film was present, it was physically removed. The specimen was then removed and re-weighed for both wet and dry weights to assess approximate tissue loss to decay. Qualitative visual assessments were scored from photographs, and replicates were terminated at sampling.

Klompmaker, Portell, and Frick 2017

In the Klompmaker et al. (2017) study, seven diverse crustaceans (calico crab, swimming crab, hermit crab, shrimp, barnacle, stomatopod, and lobster) and one chelicerate (horseshoe crab) were chosen as test subjects to assess the relative preservation potential of different marine arthropods under consistent conditions. To assess decay, ten morphological characters were taphonomically categorized with the assignment of a qualitative numerical scoring system, as follows by category:

- 1. Soft-tissue presence, 0 = all present, 1 = some, 2 = none
- 2. Cuticle coloration, 0 = original, 1 = faded, 2 = discolored/white
- 3. Separation of abdomen and carapace, 0 = no, 1 = yes
- 4. Carapace completeness, 0 = intact, 1 = abundant fragments, 2 = few fragments, 3 = no fragments
- 5. Carapace translucency, 0 = no, 1 = yes
- and 7. Claw completeness and Other appendage completeness, 0 = whole, articulated, 1 = disarticulated, nearly whole, 2 = badly fragmented, 3 = absent
- 8. Appendage translucency, 0 = no, 1 = yes
- 9. Abdomen completeness, 0 = whole, articulated, 1 = disarticulated, nearly whole, 2 = badly fragmented, 3 = absent
- 10. Telson completeness, 0 = intact, 1 = fragmented, 2 = absent.

All organisms were euthanized by freezing in fresh water for 20 hours. Specimens were placed on the bottom of a glass saltwater aquarium with continuous flow-through of artificial seawater. Specimens were not handled at any point during the experiment. Any microbial growth was left in place. Specimens were observed and photographed approximately three times a week for three months and then once a week for a total of 205 days. Qualitative visual assessments were scored from these photographs.

MATERIALS AND METHODS

To test the applicability of μ CT methods for decay experimentation, this study used *Lysmata wurdemanni* (common name: peppermint shrimp) as a model organism. Shrimp were chosen as decay subjects because they are inexpensive, easily obtained and maintained in lab aquaria, small in size, and, most importantly, have been model organisms in numerous previous decay studies (Plotnick 1986; Allison 1988; Briggs and Kear 1994; Sagemann et al. 1999; Klompmaker et al. 2017). Indeed, the model organisms from all of these studies fall within the decapod Infraorder Caridea, with the exception of Klompmaker et al. (2017) who used the decapod *Penaeus duorarum*, a member of the prawn Suborder Dendrobranchiata. The methods presented herein, however, can be applied to a wide variety of organisms, tissue types, and experimental conditions—restricted only by the scanning size parameters of the μ CT instrument being utilized.

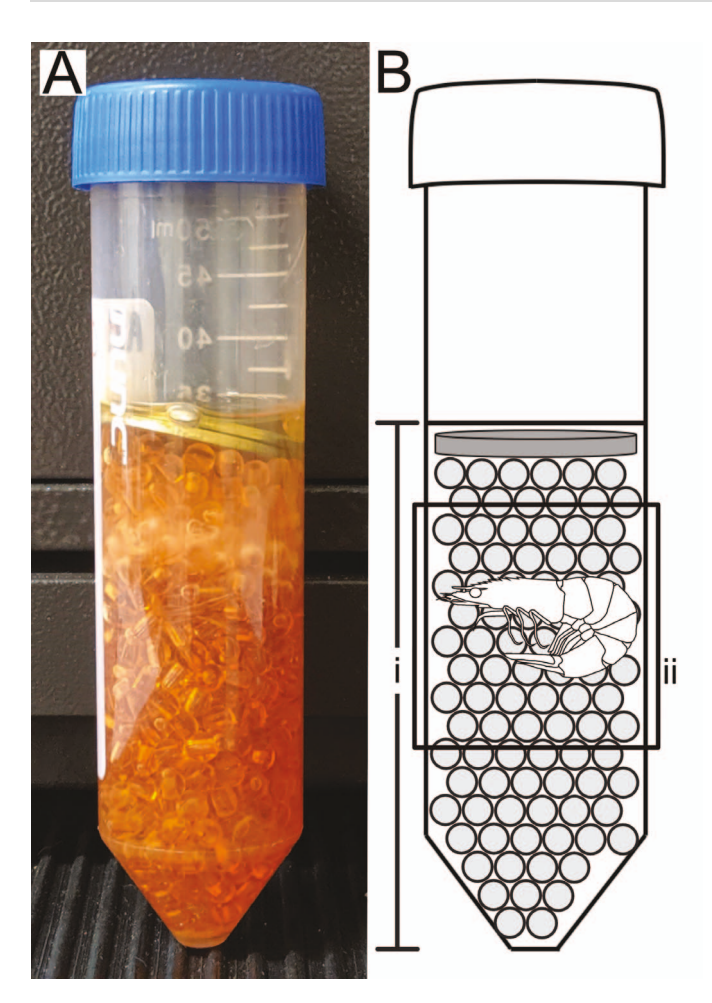


Fig. 1.—Sample preparation for decay experimentation and subsequent microcomputed tomography. **A)** Light photograph. **B)** Schematic; i = water level; ii = scanned region. Centrifuge tube is 50 ml volume, approximately 25 mm in diameter.

Decay Experimental Design

Shrimp < 50 mm in length were euthanized by asphyxia by placing them into a 1:1 solution of magnesium chloride hexahydrate and artificial seawater (Instant Ocean®, Aquarium Systems) from a stock aquarium for five minutes. Following euthanasia, the shrimp were thoroughly rinsed with artificial seawater to remove any excess magnesium chloride. To prepare the individual decay vessels for analysis, 50 ml plastic centrifuge tubes were partially filled with low-density 4 mm plastic beads to replicate high porosity sediment, followed by the specimen, more beads, and a 25mm diameter stainless steel washer placed at the top to prevent movement from the buoyancy of the beads. The washers were cleaned prior to use to remove any manufacturing chemicals or grease. The vessels were then filled with artificial seawater containing a natural host of microbes from the stock aquarium, and lightly capped to allow for air exchange (Fig. 1). A single sample was scanned immediately following euthanasia and decayvessel preparation to provide a volume and visualization of the pre-decay, pristine state. All 20 samples, including the pre-decay scanned sample, were then allowed to naturally decay under aerobic conditions. A single individual was removed from the decay sequence for µCT analysis every day for the first week, every three days up until the end of the first month, and once a week until the end of the experiment at nine weeks.

After the allotted duration of decay but prior to µCT scanning (with the exception of the pre-decay scanned sample), samples were stained with a Lugol's iodine (1% iodine metal + 2% potassium iodide—I₂KI) and 70% ethanol solution (in a 1:1 ratio; hereafter I2KI staining) as a means of enhancing soft-tissue contrast for µCT visibility. This method, known as diffusible iodine-based contrast-enhanced computed tomography (or diceCT) (Fig. 2), has become a standard anatomical practice for revealing soft tissues during µCT scanning. A wealth of published works examining the efficacy of various iodine staining methods and solutions, including for instance I₂KI, I₂E (iodine-ethanol), and I₂M (iodine-methanol), exists within the anatomical literature (e.g., Metscher 2009; Jeffrey et al. 2011; Holliday et al. 2013; Vickerton et al. 2013; Gignac et al. 2016; Li et al. 2016; Orbson et al. 2018; Sellers et al. 2017; Dickson et al. 2019, among numerous others). We encourage readers interested in using this technique to consult these works, for example the review provided by Gignac et al. (2016) and the methodology article by Metscher (2009), in order assess standards and practices and to determine the best protocol for their given samples. For our I2KI staining protocol, we began by extracting the artificial seawater from the base of the decay vessel using a 50 ml glass

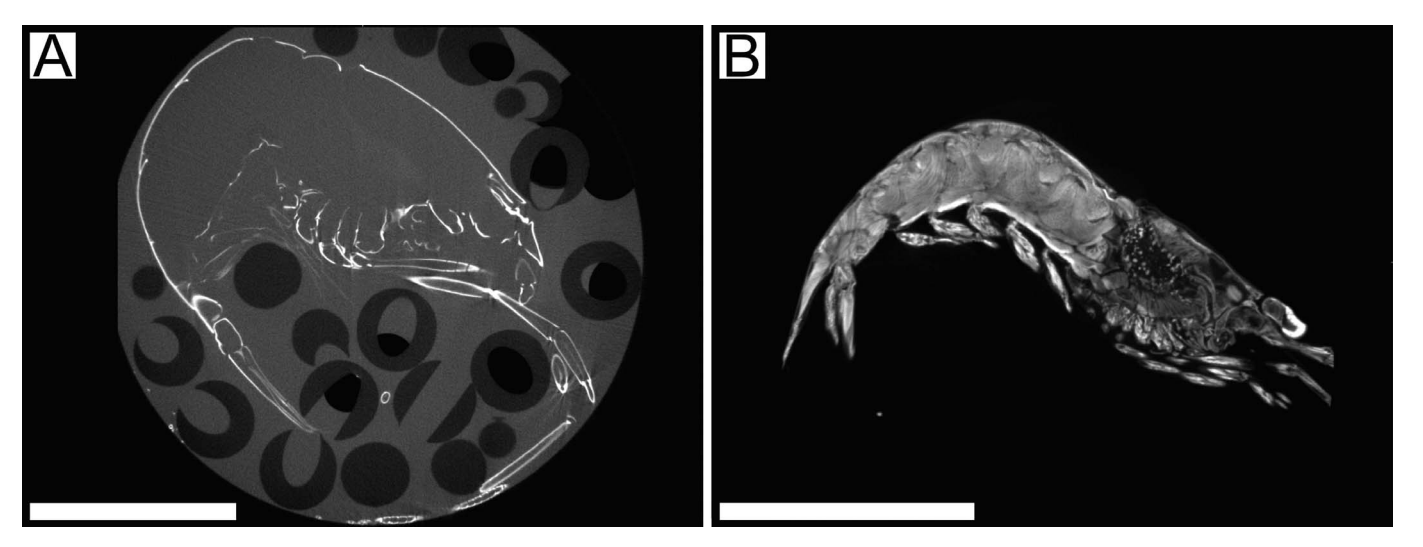


Fig. 2.—µCT 2D slice images of Lysmata wurdemanni depicting contrast differences. A) Unstained. B) I₂KI strained. Scale bar = 1 cm.

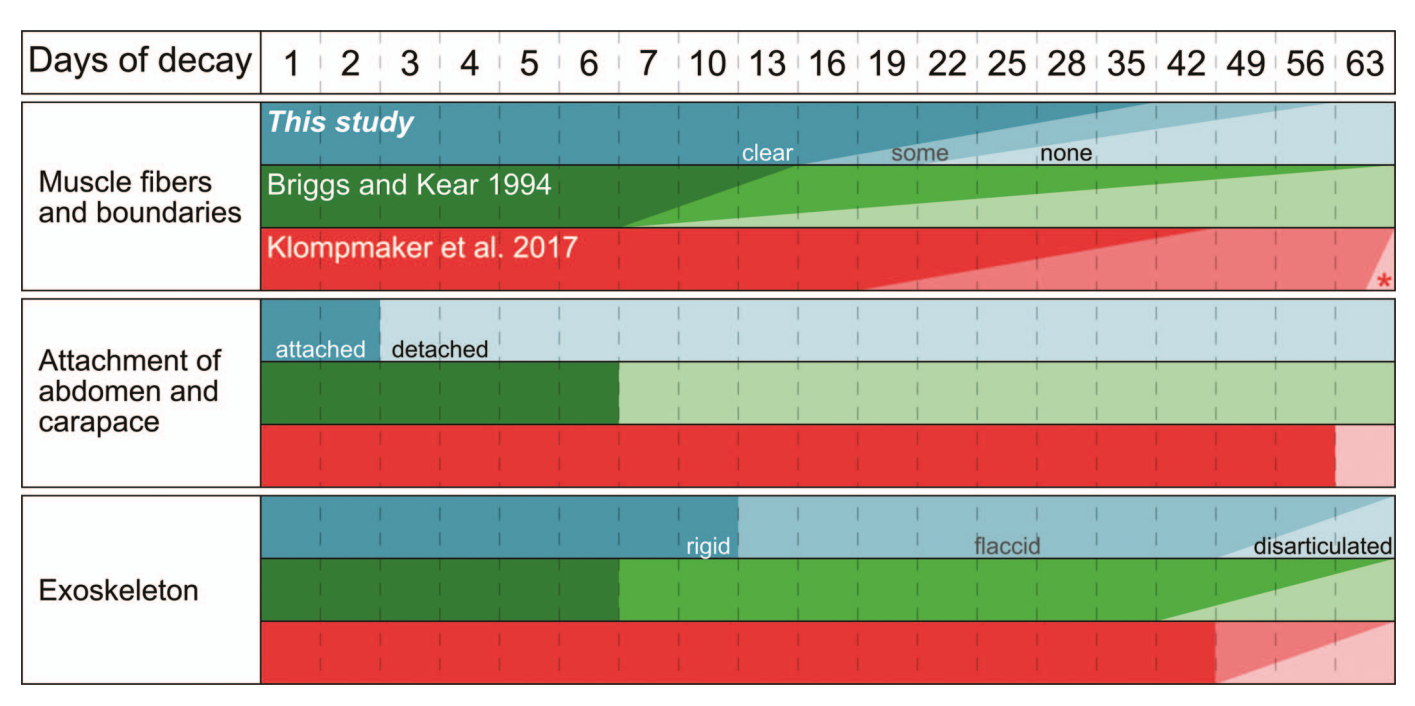


Fig. 3.—Comparison of decay indices from previous studies including data from this study (peppermint shrimp-blue); Briggs and Kear 1994 (common shrimp-green), and Klompmaker et al. 2017 (pink shrimp-red). Asterisk indicates data reported after 63 days.

Luer-lok syringe with a 5-inch needle. Using the same syringe, 10 ml of the I_2KI solution was added to the decay vessel. After being immersed for 24 hours, the same process was repeated to remove the I_2KI solution and replace 10 ml of artificial seawater prior to μ CT scanning. As an important note, the concentration and interval of interaction between the I_2KI solution and our samples was tested by trialing different concentrations and durations on undecayed shrimp replicates in order to avoid overstaining of the decayed replicates. Too much time, for example, can cause: (1) different types of tissues to become more stained than others, which may be worth consideration when targeting specific anatomical structures (Gignac et al. 2016), and (2) tissue shrinkage, thereby altering volumetric assessments or feature change (Vickerton et al. 2013).

All samples were scanned at the X-ray Microanalysis Core Facility at the University of Missouri using a Zeiss Xradia 510 Versa μCT system. Samples were scanned at optimal settings identified for the decay vessels used in this study based on 30–35% transmittance values. Our operating conditions were as follows: beam voltage = 80 kV, beam wattage = 7W, filter = LE3, exposure = 1–2 seconds (depending on transmittance), projections = 2001, and voxel size = 17.5–26.9 μm (depending on the size of the shrimp replicate). We must stress, however, that care must be taken to ensure optimum scan settings for any follow-up study based on the instrumentation and decay subjects used.

Data Analyses

The resulting data were imported to the 3D visualization software Dragonfly 2019 4.0 (Object Research Systems, Montreal, Canada) for general assessment, segmentation and volumetric analyses, and comparison with previously used decay indices. A general assessment was performed to first note which anatomical features can be visualized using μ CT and under which conditions (stained vs. unstained). Over the course of the experiment, we then observed the order and progression of decay in different anatomical structures. Next, anatomies of interest were segmented based on defined density ranges calculated from the raw tomographic data collected from the μ CT. These variations in density allow for different

anatomical structures to be selected and measured. A volumetric analysis was performed on the single individual scanned immediately after euthanasia and again using the contrast agent after 42 days of decay to assess volumetric change within one individual. The exoskeleton was segmented from the undecayed and unstained sample to interpret a sample volume. The post-decay sample was stained with $\rm I_2KI$ contrast enhancer to enable detection of soft-tissues which were then segmented for a final volume. Anatomical characters were then identified for the purpose of creating a decay index to compare μCT data to those of the previous methods outlined above.

Comparison of Decay Indices

To determine observable similarities and differences between our approach and previous studies, our resulting µCT data and visualizations were characterized using the assessment criteria established by Briggs and Kear (1994) and Klompmaker et al. (2017). To provide the most direct comparison, only data from shrimp and prawn taxa and their anatomical characters which overlapped from both decay indices were utilized in this report. We used the data from Briggs and Kear's (1994) experimental run of 50% oxygenic artificial seawater at the onset of the study followed by rapid diffusion of atmospheric gases (replicates of experimental setting 1a as described above, see their figure 2), and using Crangon crangon (common shrimp) as the decay subject. This experimental setting was explicitly chosen because it was most similar to the natural settings considered in this study and that of Klompmaker et al. (2017). From Klompmaker et al. (2017), we only assessed data from their prawn taxon, Penaeus duorarum (pink shrimp), and only from select categories of data assessment. Anatomical characters were organized by feature and include three categories, for which qualitative indices had been established in the previous publications (all quotations used below indicate terminology used in Fig. 3):

 Muscle fibers and boundaries, defined by visibility as 'clear', moderate ('some' muscle fibers/boundaries 'clear', others not), or 'none' (where muscle fibers/boundaries are homogenized).

- 2. The state of attachment ('attached' or 'detached', where attached is the primary and detached the secondary state) of the abdomen (abdominal exoskeleton) and carapace (cephalothorax exoskeleton).
- The structural integrity of the exoskeleton, defined as 'rigid' (the firm, primary state), 'flaccid' (a secondary state capable of passive deformation), and/or 'disarticulated' (an advanced state where the exoskeleton has become disjointed).

The decay index format of this report is based on that of Briggs and Kear (1994) (see details above in Previous Approaches). These same criteria were then applied to data collected from this study as well as the raw data from selected categories (1. Soft-tissue presence; 3. Separation of abdomen and carapace; 9. Abdomen completeness) from Klompmaker et al. (2017) and are reported in Figure 3. Briggs and Kear (1994) do not elaborate on what constitutes the difference between 'clear', 'somewhat clear', and 'absent' muscle fibers and boundaries; for transparency in our reporting, we have applied the following criteria: muscle fibers are neatly bundled and their boundaries are well-defined (< 50% decay, 'clear'); muscle fibers become unorganized as they deteriorate and their boundaries are less well-defined (50–90% decay, 'some'), or muscle fibers become homogenized and no boundaries are detectable (> 90% decay, 'none').

RESULTS

General Assessment

Data from μ CT scans of unstained shrimp show easily distinguishable surfaces of the exoskeleton, but soft-tissue details are minimal to undetectable. Once I_2 KI contrast stained, however, the internal anatomical features of the shrimp are observable with high-resolution detail. Using our chosen staining protocol, no staining artifacts, such as tissue shrinkage/deformation, were detected.

While our primary intent with decay tracking is to report observations comparable to previous studies, we did observe numerous other trends over the duration of the experiment. The observed progression of decay is as follows. The first sign of decay was observed on day two, as the soft tissues had begun to retract from the exoskeleton, leaving a gap in-between. On day three, the tubules of the hepatopancreas (digestive gland) began to lose definition. Also on day three, the membrane connecting the abdominal exoskeleton to the carapace ruptured, allowing the two segments to detach. By day six, exoskeleton separation between the abdomen and carapace was ubiquitous, and gill filament identification became challenging. The gills become fully unrecognizable by day 10. After 13 days, the exoskeleton began to lose rigidity and became flaccid, deforming under the weight of the washer-pinned plastic beads. Until this point, muscle fibers and their boundaries had also remained 'clear', although they began to lose definition at day 16—persisting in the 'some' visible boundaries condition until day 56. In some larger samples, however, 'clear' muscles persisted up to day 35. Day 16 also reported the loss of the nerve cord of the shrimp. The earliest sample that illustrated homogenization of the muscle tissues was that scanned on day 22, with other samples showing 'some' to 'none' throughout the remainder of the 63-day experiment. Occurring later in the experiment, the exoskeleton began experiencing multiple points of disarticulation by day 49, primarily in the legs, claws, and eye stalks (Figs. 3, 4).

Segmentation and Volumetric Analysis

To highlight the efficacy of μ CT as a useful tool for observing the sequence of decay, the muscle tissue and exoskeleton of the abdomen of the shrimp were chosen for segmentation. The abdomen of the shrimp was selected as it is comprised of primarily lower-density muscle tissues encased by the higher-density exoskeleton, making it ideal for segmentation analysis, decay tracking, and volumetric assessment. The undecayed

and unstained shrimp reported an initial abdomen volume of 975.94 mm³. After 42 days of decay, this same sample was stained and rescanned, and reported a final abdomen volume of 358.23 mm³. This is a measured loss of 617.71 mm³, or retention of 36.7% of the initial abdominal volume (Figs. 5, 6). This technique of performing pre- and post-experiment scans for volumetric comparison of freshly deceased to post-experiment individuals could be applied to other specific anatomical structures, or the entirety of the organism to assess full-body volume retention and loss.

Decay Index Comparison

For the following subsections, a brief description of the relative timing, in sequence, for the characterization of across-study indices will be listed, following the visual representation in Figure 3.

Muscle Fibers and Boundaries.—Briggs and Kear (1994) reported that well-defined, 'clear' muscle fibers and boundaries endured when the replicate was observed at the two-week mark, while this study found they persisted until day 35, and Klompmaker et al. (2017) reported them up to day 42. Briggs and Kear (1994) note that 'some' muscle fibers and boundaries had deteriorated by day seven and remained in this state throughout the duration of the experiment. Deteriorated muscles receiving the 'some' score are next reported on day 16 by this study, followed by Klompmaker et al. (2017) on day 19. At the onset of deteriorated muscles on day seven, Briggs and Kear (1994) also report the co-occurrence of homogenized ('none') muscle fibers and boundaries throughout the remainder of the experiment. We report homogenized muscles from our replicates beginning on day 22, followed by Klompmaker et al. (2017) on day 90 (denoted on Fig. 3 with an asterisk to indicate that this occurred beyond the data-reporting cut-off from this study and the Briggs and Kear study).

Separation of Abdomen from Cephalothorax.—This study reports the earliest occurrence of the decay-induced rupture of shrimp membranes connecting the abdominal exoskeleton to the carapace, allowing for the detachment of the abdomen from the cephalothorax at three days of decay, followed by Briggs and Kear (1994) at seven days, and Klompmaker et al. (2017) at 63 days. For this category, we only included two possible character states, as either 'attached' or 'detached' with no partially attached option. In all cases, once separation or detachment was first noted, it appeared at all subsequent observation times.

Exoskeleton.—Briggs and Kear (1994) report the onset of flaccidity of shrimp exoskeletons on day seven, while this study first noted flaccidity on day 13, followed by Klompmaker et al. (2017) on day 49. Exoskeletal disarticulation was reported in all three datasets at similar times, with Briggs and Kear (1994) occurring on day 42, followed by both this study and Klompmaker et al. (2017) reporting on day 49 (Figs. 3, 4).

DISCUSSION

As described above, the results from this study fall well within the same temporal range as previously reported for comparable experiments (Briggs and Kear 1994; Klompmaker et al. 2017). When applying the decay index established by Briggs and Kear (1994) and monitoring the progression of decay across features examined in all three studies, we do observe somewhat similar results—even considering the differences in the design of these studies. For example, while the Klompmaker et al. (2017) study provided less restriction on the conditions in which decay was taking place, being in open-circulatory/flow-through tanks, the Briggs and Kear (1994) study, on the other hand, was designed to evaluate strictly controlled atmospheres, although with substantially more sample handling. As compared to the hands-off approach used by Klompmaker et al. (2017),

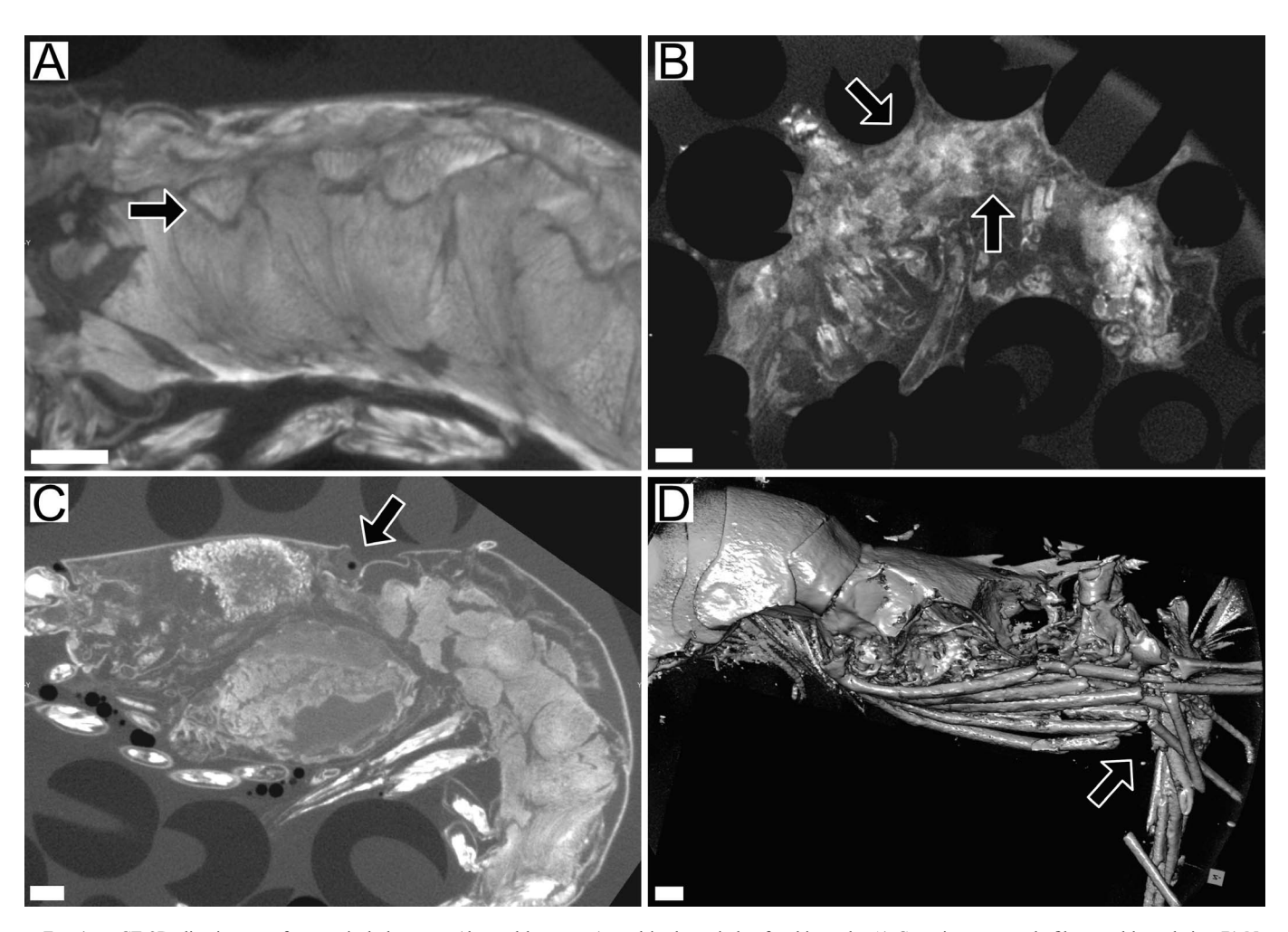


Fig. 4.— μ CT 2D slice images of anatomical characters (denoted by arrows) used in decay index for this study. **A)** Conspicuous muscle fibers and boundaries. **B)** No identifiable muscle fibers and boundaries and flaccid exoskeleton. **C)** Abdomen separated from cephalothorax. **D)** exoskeleton disarticulated. Scale = 1 mm.

physical manipulation of the decayed samples, such as removal of bacterial films, may have artificially influenced the observable state of decay and disarticulation, and contributed to decay feature states appearing earlier in the course of the experiment (Briggs and Kear 1994). The hands-off approach (Klompmaker et al. 2017) is not necessarily without its concerns, however, as the resolution of some decay-induced change may not be entirely visible without sample handling, for instance, exoskeletal flaccidity or abdomen-cephalothorax membrane rupture and separation. At least with regard to the latter, it is somewhat surprising that exoskeletal separation was not observed earlier in the course of the experiment given the freezing method (and inherent soft-tissue expansion) of euthanasia. We suggest that variation in the timing of decay-induced change is thus most likely attributable to these differences in experimental design and protocol, rather than to either the organisms used or the qualitative tracking indices. Therefore, finding similar results at least lends credence to the previously used qualitative indices, though we believe that the improved resolution offered by our µCT approach does provide a step beyond what has been previously afforded by general conventions.

Even so, application of μ CT also poses its own limitations. As we had initially anticipated, scanning of unstained shrimp (such as the pristine-state specimen) reveals that the exoskeleton has a higher relative density and X-ray attenuation as compared to the internal organs and tissues, which in turn yields little-to-no observable signal from the viscera and musculature (Fig. 2). This is unfortunately one major caveat in the

application of µCT scanning to biological specimens: the necessity of contrast enhancement for soft-tissue visualization. In our case, tissue staining via I2KI is a simple, cost-effective, and suitable means of increasing density, and therefore contrast, of the low-absorbing soft tissues-and one that can produce positive results with numerous other biological specimens (e.g., Gignac et al. 2016). Once shrimp replicates were stained, internal anatomical structures capable of detection at the set resolution became readily identifiable—in our case, offering highresolution details to categorize muscle tissue fibers and outer membranes. Once stained, the progression of decay of targeted internal soft-tissue structures became fully observable. Nevertheless, while tissue staining can be highly effective, it can also inhibit or otherwise alter the decay process. For instance, the I₂KI staining agent used herein also has antiseptic properties, and therefore halts microbially induced decay upon staining. As a result, once a replicate is stained and scanned, no further decay study could be conducted on that replicate. Thus, our resulting time-series necessarily comprises volumes of different replicates, owing to the contrast-enhancement staining procedure. Other complications can also occur with staining, and thus the emphasis on careful evaluation of staining protocol. For example, if overstained, iodine solutions can cause soft tissues to shrink, thus artificially deforming specimens and potentially affecting interpretation on the progression of decay. Even with these caveats noted, we advocate that the benefits of high-resolution 3D datasets

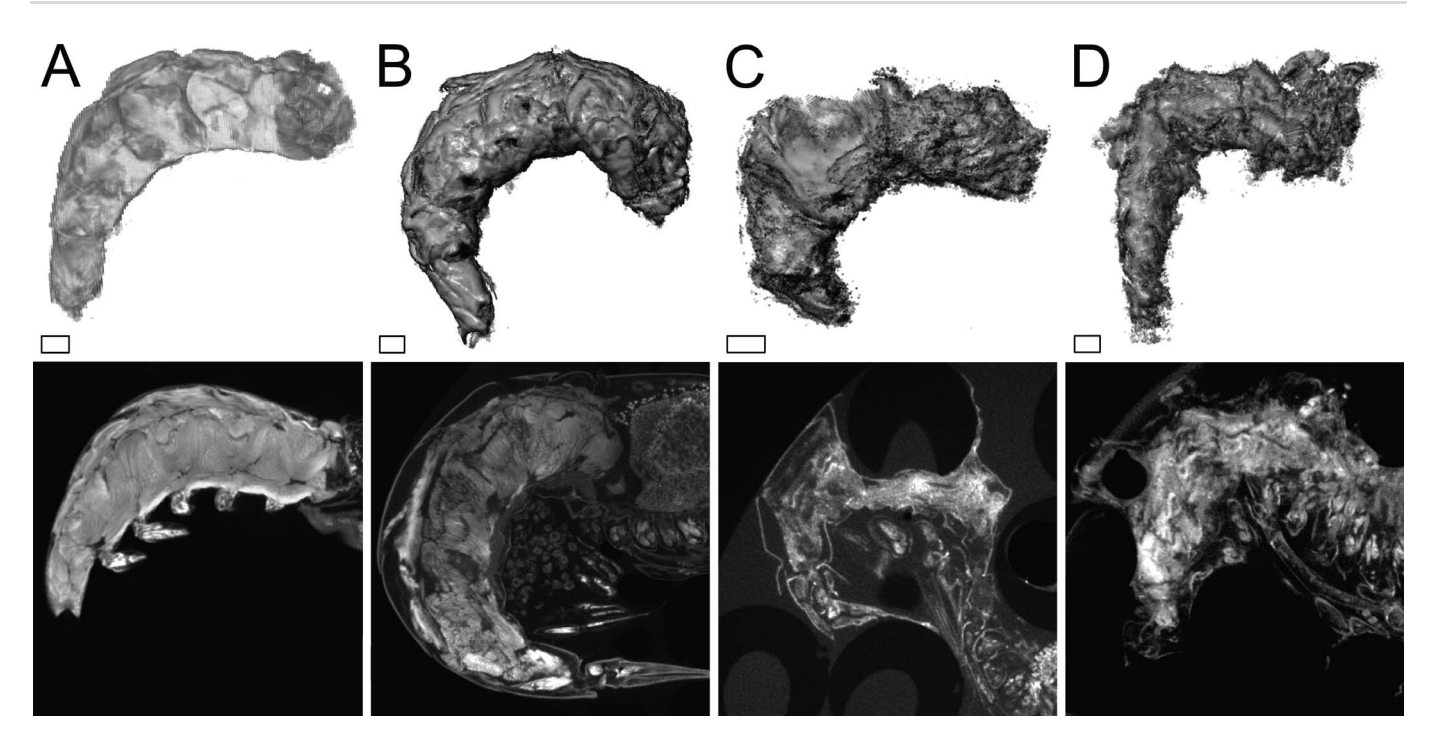


Fig. 5.— μ CT 3D segmented abdominal muscles (top row) and 2D slice images (bottom row) at vary days of decay. **A**) 0 days. **B**) 7 days. **C**) 16 days. **D**) 63 days. Scale = 1 mm.

allowable by soft-tissue staining outweigh the inherent limitations of staining when appropriate specimen-dependent protocols are utilized.

While the μ CT scans of the freshly killed and unstained shrimp show details of only the exoskeleton of the specimen, with internal features minimally observable or unresolvable, these data are still useful for ascertaining the pre- and post-decay specimen volumes, and thus volume loss or retention over the course of decay. While in our case, pre- and post-experiment scanning was limited to only one individual for validation purposes, we propose that—if volume and mass change are targeted metrics—scanning of pre- and post-decay replicates may be important steps in follow-up experimentation. To maximize time efficiency between scanning replicates, batches of organisms can be scanned together

immediately following euthanasia. If properly conducted, this technique can be applied regardless of the target taxon, as μ CT will capture the external isosurface of the sample due to the density difference between the sample and surrounding air or liquid. From comparison of initial, unstained isosurfaces to volumetric and anatomical analysis of the stained, post-decay specimens, one can surmise by distortion or absence of internal structures where decay had the most pronounced effect. One consideration to be mindful of, however, with regard to pre- and post-decay scanning of the same individuals is the potential effect of X-radiation on the gut and other organism-associated microbiota, which may contribute to decay of the organism. Turning to the soil literature for insights on this concern yields contradictory results: several studies suggest negligible effects of X-

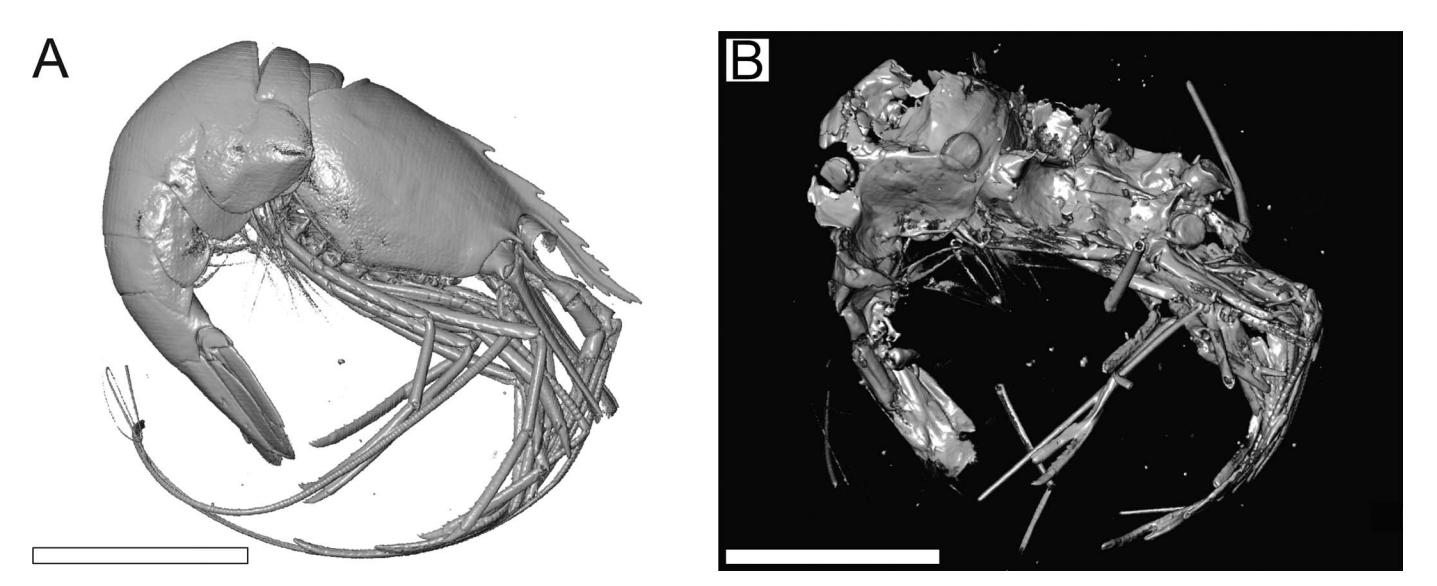


Fig. 6.—µCT 3D isosurface renderings of Lysmata wurdemanni. A) Unstained specimen at day 0. B) Stained specimen at 42 days of decay. Scale bar = 1 cm.

radiation on μ CT-scanned soil microbes (Bouckaert et al. 2013; Zappala et al. 2013; Schmidt et al. 2015), whereas another revealed a much more detrimental effect in microbial biomass and community structure (Fischer et al. 2013). While high-dose X-radiation indeed has been shown as a viable mechanism for food decontamination (Mahmoud 2012), for example, such doses are substantially greater than those imparted during μ CT scanning. Nonetheless, while we did not control for this concern, refreshing the replicates with stock aquarium seawater, for example, might be a useful step for re-inoculation following the initial pre-decay scan.

Perhaps the greatest benefit of applying µCT in decay experiments is the augmented ability to reveal the integrity or fragility of anatomical structures, allowing for visibility of decay in previously unobservable, internal features. A prime example of this improvement comes during the observation of the abdomen and cephalothorax, where we could virtually dissect and visualize rupture of the membrane that would allow for the detachment of the abdomen from the cephalothorax prior to its actual or observed separation. When compared to our benchmark studies, we were able to detect this decay-state four days before it is observed by Briggs and Kear (1994) and two months before Klompmaker et al. (2017). Our tomographic methodology makes it possible to identify whether the connective membrane between these anatomical structures is intact, importantly without sample movement which could result in rupture or detachment and thus skew the interpretation towards a more decayed state. That Klompmaker et al. (2017) did not report separation of the cephalothorax and abdomen until much later likely results from their observation in situ, and thus not recording this change in character state until they became conspicuously disarticulated.

CONCLUSIONS

While the results of these three studies were able to be presented via merged qualitative scoring indices, it is apparent that such methodologies fall short in capturing the entire picture of decay. We note that the pilot data in this study are limited, but we demonstrate that utilizing µCT for 3D visualization of taphonomic experiment replicates can be an effective and practical technique for monitoring the progression of decay. This approach can be even more effective when coupled with contrast-enhancement staining to provide visibility of soft tissues. Using the methodology as described herein, we were able to capture and inspect 3D views, including virtual dissection of internal anatomical structure, of entire post-decay organisms at high resolution with minimal physical sample manipulation or movement. This approach thus overcomes limitations imposed either by possibly destructive sample handling (Briggs and Kear 1994) or obscured visibility from minimal handling (Klompmaker et al. 2017), and instead augments our ability to systematically track decay with previously unseen and undisturbed detail. In comparison with previous experiments using similar organisms, our data show a consistent pattern of anatomical change from decay with those reports. While this does lend support for the value of qualitative decay scoring indices, their subjective nature and tendency to shoehorn data into defined categories based on the mode of replicate observation proves difficult for their direct and consistent application to

We suggest that utilizing μ CT as a means to track and characterize experimental decay over time may thus provide a more holistic, broadly applicable, and repeatable approach across numerous study designs. Perhaps most importantly, if this methodology can become more widely adopted, the ability to share digital datasets, for instance comprising the entire volume of scanned organisms, holds promise for enhanced comparability and assessment between a multitude of studies—and unlocking meaningful correlation of taphonomic histories of organisms across a range of study conditions. Once the full volume datasets are captured, later segmentation and processing software can be used to isolate targeted anatomical structures for more exact tracking of sequential decay-

induced change, along with several other assessments such as (but not exhaustively) tractography of muscle fibers, rate of compaction, decayinduced loss of structural integrity, resulting tissue collapse and distortion, and propagation of mineralization—all of which would of course need to be tailored to the specificities of future taphonomic studies and testing their given hypotheses. In sum, we encourage the adoption of μCT for decay tracking as this method affords researchers the ability to examine decay products across an immeasurably wide range of experimental designs. Its high-resolution 3D views establish it as a reliable means for appraising the factors that influence decay and, by extrapolation, impact our view of the fossil record.

ACKNOWLEDGMENTS

The authors thank Evan Anderson (University of Missouri) for assistance with data collection and Brock Andreasen (University of Missouri) for assistance with data processing and segmentation. We are additionally grateful to the constructive reviews provided by Brandt Gibson and an anonymous reviewer. This research was supported by the Paleontological Society Norman Newell Early Career Grant (TS); the National Science Foundation EAR CAREER 1652351 (JDS); and NSF EAR Instrumentation & Facilities 1636643 (JDS, TS).

TS and JDS are responsible for the conception of this project and methodological design; TS collected and processed the data; TS and JDS interpreted the data, constructed the figures, and wrote the manuscript.

SUPPLEMENTAL MATERIAL

The raw data files for all 20 scanned shrimp used in this study, segmented Dragonfly data (.ORSSession files), and supplemental video files are available for download.

Data are available from the PALAIOS Data Archive: https://www.sepm.org/supplemental-materials.

REFERENCES

Allison, P.A., 1988, The role of anoxia in the decay and mineralization of proteinaceous macro-fossils: Paleobiology, v. 14, p. 139–154, doi: 10.1017/S009483730001188X.

Behrensmeyer, A.K. and Kidwell, S.M., 1985, Taphonomy's contributions to paleobiology. Paleobiology, v. 11, p. 105–119, doi: 10.1017/S009483730001143X.

BOUCKAERT, L., VAN LOO, D., AMELOOT, N., BUCHAN, D., VAN HOOREBEKE, L., AND SLEUTEL, S., 2013, Compatibility of X-ray micro-computed tomography with soil biological experiments: Soil Biology and Biochemistry, v. 56, p. 10–12, doi: 10.1016/j.soil bio.2012.02.002.

Briggs, D.E.G., 1995, Experimental taphonomy: PALAIOS, v. 10, p. 539–550, doi: 10.230 7/3515093.

Briggs, D.E.G., 2003, The role of decay and mineralization in the preservation of soft-bodied fossils: Annual Review of Earth and Planetary Sciences, v. 31, p. 275–301, doi: 10.1146/annurev.earth.31.100901.144746.

BRIGGS, D.E.G. AND KEAR, A.J., 1993, Decay and preservation of polychaetes: taphonomic thresholds in soft-bodied organisms: Paleobiology, v. 19, p. 107–135, doi: 10.1017/S00 94837300012343.

BRIGGS, D.E.G. AND KEAR, A.J., 1994, Decay and mineralization of shrimps: PALAIOS, v. 9, p. 431–456, doi: 10.2307/3515135.

CAI, Y., SCHIFFBAUER, J.D., HUA, H. AND XIAO, S., 2012, Preservational modes in the Ediacaran Gaojiashan Lagerstätte: pyritization, aluminosilicification, and carbonaceous compression: Palaeogeography, Palaeoclimatology, Palaeoecology, v. 326, p. 109–117, doi: 10.1016/j.palaeo.2012.02.009.

Darroch, S.A.F., Laflamme, M., Schiffbauer, J.D., and Briggs, D.E.G., 2012, Experimental formation of a microbial death mask: PALAIOS, v. 27, p. 293–303, doi: 10.2110/palo.2011.p11-059r.

DICKSON, E., BASHAM, C., RANA, A., AND HARTSTONE-ROSE, A., 2019, Visualization and quantification of digitally dissected muscle fascicles in the masticatory muscles of *Callithrix jacchus* using nondestructive diceCT: The Anatomical Record, v. 302, p.1891–1900, doi: 10.1002/ar.24212.

FISCHER, D., PAGENKEMPER, S., NELLESEN, J., PETH, S., HORN, R., AND SCHLOTER, M., 2013, Influence of non-invasive X-ray computed tomography (XRCT) on the microbial community structure and function in soil: Journal of Microbiological Methods, v. 93, p. 121–123, doi: 10.1016/j.mimet.2013.02.009.

FORDYCE, A.J., KNUEFING, L., AINSWORTH, T.D., BEECHING, L., TURNER, M., AND LEGGAT, W., 2020, Understanding decay in marine calcifiers: micro-CT analysis of skeletal structures

- provides insight into the impacts of a changing climate in marine ecosystems: Methods in Ecology and Evolution, v. 11, p. 1021–1041, doi: 10.1111/2041-210X.13439.
- GIBSON, B.M., SCHIFFBAUER, J.D., AND DARROCH, S.A.F., 2018, Ediacaran-style decay experiments using mollusks and sea anemones: PALAIOS, v. 33, p. 185–203, doi: 10.2110/palo.2017.091.
- GIGNAC, P.M., KLEY, N.J., CLARKE, J.A., COLBERT, M.W., MORHARDT, A.C., CERIO, D., COST, I.N., COX, P.G., DAZA, J.D., EARLY, C.M., ECHOLS, M.S., HENKELMAN, R.M., HERDINA, A.N., HOLLIDAY, C.M., LI, Z., MAHLOW, K., MERCHANT, S., MÜLLER, J., ORSBON, C.P., PALUH, D.J., THIES, M.L., TSAI, H.P., AND WITMER, L.M., 2016, Diffusible iodine-based contrast-enhanced computed tomography (diceCT): an emerging tool for rapid, high-resolution, 3-D imaging of metazoan soft tissues: Journal of Anatomy, v. 228, p. 889–909, doi: 10.1111/joa.12449.
- HOLLIDAY, C.M., TSAI, H.P., SKILJAN, R.J., GEORGE, I.D., AND PATHAN, S., 2013, A 3D interactive model and atlas of the jaw musculature of *Alligator mississippiensis*: PLoS ONE, 8:e62806, doi: 10.1371/journal.pone.0062806.
- INIESTO, M., LAGUNA, C., FLORÍN, M., GUERRERO, M.C., CHICOTE, A., BUSCALIONI, A.D., AND LOPEZ-ARCHILLA, A.I., 2015, The impact of microbial mats and their microenvironmental conditions in early decay of fish: PALAIOS, v. 30, p. 792–801, doi: 10.2110/palo.2014.086.
- JEFFERY, N.S., STEPHENSON, R.S., GALLAGHER, J.A., JARVIS, J.C., AND COX, P.G., 2011, Micro-computed tomography with iodine staining resolves the arrangement of muscle fibres: Journal of Biomechanics, v. 44, p. 189–192, doi: 10.1016/j.jbiomech.2010.08.027.
- KLOMPMAKER, A.A, PORTELL, R.W., AND FRICK, M.G., 2017, Comparative experimental taphonomy of eight marine arthropods indicates distinct differences in preservation potential: Palaeontology, v. 60, p. 773–794, doi: 10.1111/pala.12314.
- LI, Z., KETCHAM, R.A., YAN, F., MAISANO, J.A., AND CLARKE, J.A., 2016, Comparison and evaluation of the effectiveness of two approaches of diffusible iodine-based contrastenhanced computed tomography (diceCT) for avian cephalic material: Journal of Experimental Zoology (Molecular and Developmental Evolution), v. 326B, p. 352–362, doi: 10.1002/jez.b.22692.
- MÄHLER, B., JANSSEN, K., MENNEKEN, M., TAHOUN, M., LAGOS, M., BIERBAUM, G., MÜLLER, C.E., AND RUST, J., 2020, Calcite precipitation forms crystal clusters and muscle mineralization during the decomposition of *Cambarellus diminutus* (Decapoda: Cambaridae) in freshwater: Palaeontologia Electronica, v. 23, doi: 10.26879/992.
- MAHMOUD, B.S.M., 2012, Effects of X-ray treatments on pathogenic bacteria, inherent microflora, color, and firmness on whole cantaloupe: International journal of Food Microbiology, v. 156, p. 296–300, doi: 10.1016/j.ijfoodmicro.2012.04.001.
- McCoy, V.E., Young, R.T., and Briggs, D.E., 2015, Factors controlling exceptional preservation in concretions: PALAIOS, v. 30, p. 272–280, doi: 10.2110/palo.2014.081.

 Metscher, B.D., 2009, MicroCT for comparative morphology: simple staining methods allow high-contrast 3D imaging of diverse non-mineralized animal tissues: BMC Physiology, v. 9, p. 11, doi: 10.1186/1472-6793-9-11.

- Orbson, C.P., GIDMARK, N.J., AND Ross, C.F., 2018, Dynamic musculoskeletal functional morphology: integrating diceCT and XROMM: The Anatomical Record, v. 301, p. 378–406, doi: 10.1002/ar.23714.
- PLOTNICK, R.E., 1986, Taphonomy of a modern shrimp: implications for the arthropod fossil record: PALAIOS, v. 1, p. 286–293, doi: 10.2307/3514691.
- Purnell, M.A., Donoghue, P.J., Gabbott, S.E., McNamara, M.E., Murdock, D.J., and Sansom, R.S., 2018, Experimental analysis of soft-tissue fossilization: opening the black box: Palaeontology, v. 61, p. 317–323, doi: 10.1111/pala.12360.
- SAGEMANN, J., BALE, S.J., BRIGGS, D.E.G., AND PARKES, R.J., 1999, Controls on the formation of authigenic minerals in association with decaying organic matter: an experimental approach: Geochimica et Cosmochimica Acta, v. 63, p. 1083–1095, doi: 10.1016/S0016-7037(99)00087-3.
- SANSOM, R.S., 2014, Experimental decay of soft tissues, in M. Laflamme, J.D. Schiffbauer, and S.A.F. Darroch (eds.), Paleontological Society Papers, v. 20, p. 259–274, doi: 10.1017/S1089332600002886.
- SANSOM, R.S., GABBOTT, S.E., AND PURNELL, M.A., 2010, Non-random decay of chordate characters causes bias in fossil interpretation: Nature, v. 463, p. 797–800, doi: 10.1038/ nature08745.
- Schiffbauer, J.D., Xiao, S., Cai, Y., Wallace, A.F., Hua, H., Hunter, J., Xu, H., Peng, Y., and Kaufman, A.J., 2014, A unifying model for Neoproterozoic–Palaeozoic exceptional fossil preservation through pyritization and carbonaceous compression: Nature Communications, v. 5, p. 1–12, doi: 10.1038/ncomms6754.
- Schmidt, H., Vetterlein, D., Köhne, J.M., and Eickhorst, T., 2015, Negligible effect of X-ray μ-CT scanning on archaea and bacteria in an agricultural soil: Soil Biology and Biochemistry, v. 84, p. 21–27, doi: 10.1016/j.soilbio.2015.02.010.
- Sellers, K.C., Middleton, K.M., Davis, J.L., and Holliday, C.M., 2017, Ontogeny of bite force in a validated biomechanical model of the American alligator: Journal of Experimental Biology, v. 220, p. 2036–2046, doi: 10.1242/jeb.156281.
- Vickerton, P., Jarvis, J., and Jeffrey, N., 2013, Concentration-dependent specimen shrinkage in iodine-enhanced micro CT: Journal of Anatomy, v. 223, p. 185–193, doi: 10.1111/joa.12068.
- WILSON, L.A. AND BUTTERFIELD, N.J., 2014, Sediment effects on the preservation of Burgess Shale–type compression fossils: PALAIOS, v. 29, p. 145–154, doi: 10.2110/palo.2013.0 75
- ZAPPALA, S., HELLIWELL, J.R., TRACY, S.R., MAIRHOFER, S., STURROCK, C.J., PRIDMORE, T., BENETT, M., AND MOONEY, S.J., 2013, Effects of X-ray dose on rhizosphere studies using X-ray computed tomography: PLOS ONE, 8:e67259, doi: 10.1371/journal.pone.0067250.

Received 22 January 2021; accepted 30 March 2021.